ANGULAR MOMENTUM IN RANDOM WALK

BY M. DWORZECKA*

Department of Physics, George Mason University, Fairfax, Virginia 22030

M. ZIELINSKA-PFABÉ

Department of Physics, Smith College, Northampton, Massachusetts 01063

AND J. J. GRIFFIN

Department of Physics and Astronomy, University of Maryland, College Park, Maryland 20742

(Received September 5, 1989)

The influence of the angular momentum on the relationship between nucleon transfer and kinetic energy loss in deep inelastic heavy ion reactions is studied within a discrete two-dimensional random walk formalism. It is found that the dependence upon the number of steps q of each of the physical quantities calculated is rather insensitive to the angular momentum. When this q-dependence is converted to energy loss, the sensitivity to L is increased and becomes more pronounced for larger values of E_{loss} becoming extreme as the energy loss approaches its maximum value for each L, reflecting the fact that in this limit more and more nucleons must be transferred to effect any given increase in the energy loss. On the other hand, this situation is not expected to occur experimentally, where large L-values are strongly correlated with small energy losses. Thus physical processes at small energy losses, where the sensitivity of the observables to angular momentum is calculably small, are associated with the largest angular momenta, whereas in processes involving larger energy losses where the observed quantities are calculated to have an increasing sensitivity to L, only small angular momenta are involved. Thus the present analysis offers quantitative support for the view that such deep inelastic processes are not very sensitive to the value of the angular momentum. We have also sought to understand the angular momentum dependences calculated as reflecting primarily the angular momentum dependence of the random walk transition probabilities. The results show that the dependence of these probabilities upon L, implicitly through their dependence upon E_{loss}, is, for large values of E_{loss}, such as to yield qualitatively the calculated dependences upon L of the several observables.

PACS numbers: 25.70.Lm

* Partially supported by National Science Foundation under grant #PHY-8704471.

1. Introduction

A discrete two-dimensional Random Walk (RW) formalism [1] has been used to study the relation between nucleon transfer and kinetic energy loss during deep inelastic heavy ion reactions. Neutrons and protons were assumed to be transferred between two interacting nuclei with transition probabilities assumed proportional to the level densities of the final states. Each such nucleon transfer is assumed to involve a certain dissipation of the kinetic energy of relative motion into heat. In order to accommodate other possible physical processes which lead to dissipation of energy by some means other than nuclear transfer, a fifth non-transfer step (in addition to the four possible transfers of proton or neutron from the projectile to the target and vice versa) has been included in the RW formalism [2]. It leads simply to a renormalization of the transition rates.

By demanding the conservation of the average linear momentum during the transfer process one can calculate the maximum energy consistent with conservation of linear momentum which becomes available for excitation energy as each nucleon is transferred, and thereby estimate the maximal kinetic energy loss per transfer. In previous calculations [1, 2] the relative angular momentum of the two fragments has been assumed to be constant with no possibility of a transfer of the relative angular momentum into internal angular momenta of the projectile and the target. Thus the two nuclei were in effect assumed to slide past one another without feeling any torques due to surface friction.

In the present paper we allow both for the rotation of the two nuclei individually about the axes through their centers and for the rotation of the whole system about its center of mass [3]. When nucleons are transferred between the projectile and the target, the angular momentum of the relative motion decreases and the summed internal angular momentum of the individual nuclei increases, conserving, of course, the total angular momentum.

The mass and charge distributions of the reaction products are then described by a family of functions of the energy loss, one for each value of the (conserved) total angular momentum, as defined initially by the impact parameter of the collision.

In Sect. 2 we present the brief description of the random walk formalism, and in Sect. 3, a derivation of the expressions for the energy loss due to nucleon transfer in a system of angular momentum, L. In Sect. 4 we present our calculated results and discuss the effects of a non-zero angular momentum on various calculated mean values and widths of the mass and charge distributions.

2. Random walk

The basic assumption of the RW approach to the nucleon transfer problem is that the (N, Z) values of the projectile-like fragment (and, complementarily, those of the target) change by a sequence of independent single-nucleon transfers through the "window" which opens between the interacting nuclei. During each transfer, a certain average linear momentum is carried from one nucleus to the other and a certain amount of energy is converted from the kinetic energy of the relative motion to internal (or heat) energy.

The probability distribution $P_q(N, Z)$ after q steps is given by

$$P_q[(N, Z)] = \sum_{\alpha=0}^{4} T_\alpha[(N, Z)-\Delta_\alpha, q]P_{q-1}[(N, Z)-\Delta_\alpha], \tag{1}$$

where $\Delta_\alpha = (0, 0), (1, 0), (0, -1), (-1,0), (0, 1)$ represents displacement vectors on the (N, Z) plane. The transition probability for $\alpha = 0$ which describes the non-transfer step is a free parameter,

$$\hat{T}_0(N, Z, q) = \gamma, \tag{2}$$

while for $\alpha = 1, 2, 3, 4$ the transition probabilities are taken to be proportional to the level density $\varrho_\alpha(E^*_\alpha)$ of final states of the total dinuclear system which can be reached after the transfer; i.e.,

$$\hat{T}_\alpha(N, Z, q) = \varrho\{E^*[(N, Z)+\Delta_\alpha], q\}, \quad \alpha = (1, 2, \ldots 4). \tag{3}$$

The transition probabilities are than normalized for insertion into (1),

$$T_\alpha(N, Z, q) = (1-\gamma)\hat{T}_\alpha(1/\sum_{\delta=1}^{4} \hat{T}_\delta). \tag{4}$$

The final state level density in (3) has been assumed to have the following exponential dependence upon $\sqrt{E^*}$,

$$\varrho(E^*) = \frac{1}{12}\left(\frac{0.25}{37}\right)^{-1/4} \frac{1}{(E^*)^{5/4}} \exp\left[2\pi\sqrt{(0.25/37)AE^*}\right]. \tag{5}$$

Here $A = A_1+A_2$ is the (constant) sum of the mass numbers of the projectile and of the target. The excitation energy E^* increases with q and is calculated as the sum of the energy dissipated by the nucleon transfer and the decrease in the ground state energy of the system,

$$E^*(N_1, Z_1, N_2, Z_2, q) = E_{\text{diss}}(q)-E_{\text{gs}}(Z_1, N_1, Z_2, N_2). \tag{6}$$

Here E_{gs} is the ground state energy of the system (with respect to the injection point, defined by the initial projectile-target projectile combination) after the q^{th} nucleon transfer and $E_{\text{diss}}(q)$ is the (cumulative) total energy dissipated into heat after q steps;

$$E_{\text{diss}}(q) = E_{\text{loss}}(q)-E^{(1)}_{\text{rot}}(q)-E^{(2)}_{\text{rot}}(q). \tag{7}$$

Here $E^{(1)}_{\text{rot}}$ and $E^{(2)}_{\text{rot}}$ are the rotational kinetic energies of the projectile and target about the axes through their centers. Also, $E_{\text{loss}}(q)$, the accummulated loss in relative kinetic energy after q steps, is given by the difference between the initial kinetic energy of the relative motion and its value after q steps;

$$E_{\text{loss}}(q) = E_{\text{k}}(0)-E_k(q). \tag{8}$$

The initial value of the kinetic energy of the relative motion in the center of mass frame is given by

$$E_{\text{k}}(0) = E_{\text{CM}}-E_{\text{Coul}}-V_{\text{Pr}}, \tag{9}$$

where the CM bombarding energy of the reaction is given by

$$E_{\mathrm{CM}} = E_{\mathrm{lab}} \frac{A2}{A1+A2}, \tag{10}$$

where E_{lab} is the kinetic energy of the projectile, A_1, in the laboratory frame. The Coulomb energy for the two touching spherical nuclei is

$$E_{\mathrm{Coul}} = \frac{e^2 Z_1 Z_2}{R_1+R_2}, \tag{11}$$

where, we use the droplet model [4] radii,

$$R_{1,2} = 1.28\, A_{1,2}^{1/3} + 0.8\, A_{1,2}^{-1/3} - 0.76. \tag{12}$$

The proximity potential [5] is given by

$$V_{\mathrm{Pr}} = -4\pi\gamma\varphi \frac{R_1 R_2}{R_1+R_2} \tag{13}$$

with

$$\gamma = 0.9517\left[1 - 1.7826\left(\frac{(N_1+N_2)-(Z_1+Z_2)}{A_1+A_2}\right)^2\right] \tag{14}$$

$$\varphi = -1.8296 \text{ MeV/fm}. \tag{15}$$

The formulas for $E_{\mathrm{k}}(q)$ and $E_{\mathrm{rot}}^{(1)}$ and $E_{\mathrm{rot}}^{(2)}$ are derived in the following Section.

3. Angular momentum formalism

3.1. Linear and angular momentum transfer

We consider a system of two interacting spherical nuclei, A_1 and A_2 in contact in the center of mass frame (see Fig. 1). The projectile-like fragment (A_1) has linear momentum P_1 in the CM of the dinuclear system and an angular momentum of L_1 about its own center of mass. For the target-like fragment, the linear momentum is $P_2 = -P_1$ and the angular momentum is L_2. We let L_{12}, analyzed in more detail below, denote the angular momentum of the relative motion of the two fragments about their common center of mass, C.

We assume that the nucleonic momenta are restricted to a plane defined by the unit radial and tangential vectors $\hat{r}$ and $\hat{t}$ in Fig. 1 and we neglect the initial spins of target and projectile. Then we can write

$$P_1 = P_{1t}\hat{t} + P_{1r}\hat{r} \tag{16}$$

and $L_{1z} = |L_1| = L_1$, $L_{2z} = L_2$, and $L_{12z} = L_{12}$ for the components of the angular momenta along the z-axis perpendicular to the plane of $\hat{t}$ and $\hat{r}$. The total angular momentum

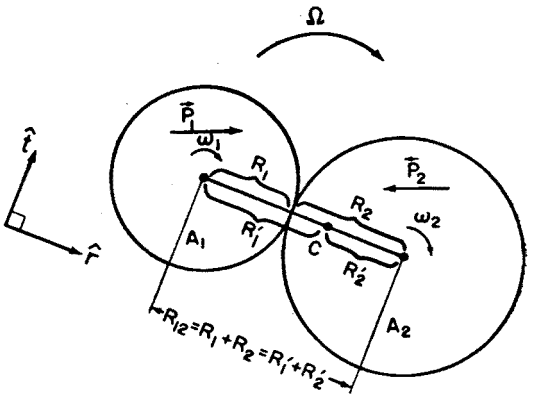

Fig. 1. Geometry of the dinuclear system

also points in this direction and is a constant of motion,

$$L = L_1 + L_2 + L_{12}. \tag{17}$$

For a system of two touching spheres we can write

$$L_1 = I_1 \omega_1, \tag{18a}$$

$$L_2 = I_2 \omega_2, \tag{18b}$$

$$L_{12} = I_{12} \Omega, \tag{19}$$

where ω_1, ω_2 and Ω denote the angular velocities around the z-axis of A_1, A_2 and of the whole system, respectively, and the rotational inertias are calculated in the rigid body limit:

$$I_1 = \tfrac{2}{5} A_1 m R_1^2, \tag{20a}$$

$$I_2 = \tfrac{2}{5} A_2 m R_2^2, \tag{20b}$$

$$I_{12} = \mu(R_1' + R_2')^2 = \mu(R_1 + R_2)^2 = \mu R_{12}^2. \tag{21}$$

In (21), $\mu = \dfrac{m A_1 A_2}{A_1 + A_2}$ is the reduced mass, R_1' and R_2' are the distances from the center of the nuclei to the common center of mass, and m is the nucleon mass.

The relative angular momentum can also be related to the linear momenta via

$$L_{12} = -P_{1t} R_1' + P_{2t} R_2'. \tag{22}$$

Using the fact that $P_2 = -P_1$ and $R_1' + R_2' = R_1 + R_2 = R_{12}$ (see Fig. 1), we may rewrite Eq. (22) as:

$$L_{12} = -P_{1t} R_{12}. \tag{23}$$

We now consider a nucleon transferred from the projectile to the target (i.e., to the right in Fig. 1). It carries with it its average share of the relative linear momentum of the projectile, namely,

$$p^+ = P_1/A_1. \tag{24}$$

Moreover, if nucleus A_1 before the transfer is rotating rigidly with the angular speed ω_1, a nucleon at the window has also an additional tangential velocity,

$$u_{1t} = \omega_1 R_1. \tag{25}$$

Therefore the radial and tangential components of the linear momentum of this nucleon as it crosses the window are

$$p_r^+ = P_{1r}/A_1, \tag{26a}$$

$$p_t^+ = m\omega_1 R_1 + (P_{1r}/A_1). \tag{26b}$$

Consequent to the transfer of this nucleon from left to right, the linear momenta of the projectile nucleus and target nucleus assume the new values

$$P_{1r}^+ = P_{1r} - p_r^+, \quad P_{2r}^+ = P_{2r} + p_r^+; \tag{27a}$$

$$P_{1t}^+ = P_{1t} - p_t^+, \quad P_{2t}^+ = P_{2t} + p_t^+; \tag{27b}$$

and the angular momentum, the new value

$$L_1^+ = L_1 - p_t^+ R_1, \tag{28a}$$

for the projectile and

$$L_2^+ = L_2 - p_t^+ R_2, \tag{28b}$$

for the target. The relative angular momentum after the transfer is

$$L_{12}^+ = L_{12} + p_t^+ R_{12}, \tag{29}$$

and one can easily verify that the total angular momentum is conserved,

$$L_1^+ + L_2^+ + L_{12}^+ = L_1 + L_2 + L_{12}. \tag{30}$$

If a particle is transferred from the target to the projectile, i.e., to the left, the components of its momentum are

$$p_r^- = -P_{1r}/A_2, \tag{31a}$$

and

$$p_t^- = -m\omega_2 R_2 - (P_{1t}/A_2), \tag{31b}$$

where we have used $P_2 = -P_1$. And again we can calculate linear and angular momenta of the two nuclei after the transfer, with results that can also be obtained from (27) and (28) replacing p^+ by p^-, and interchanging the labels 1 and 2. Likewise, the relative angular momentum is given by Eq. (29) with p_t^+ replaced by p_t^-. Again, we can easily check that the total angular momentum is conserved.

We now calculate the averages of the linear and angular momenta after one transfer in each direction (i.e., from the projectile to target and from target to projectile). For the target (1) linear momentum we obtain the results

$$\bar{P}_{1r} = P_{1r} - (p_r^+ - p_r^-)/2, \tag{32a}$$

$$\bar{P}_{1t} = P_{1t} - (p_t^- - p_t^-)/2, \tag{32b}$$

and for the angular momenta,

$$\bar{L}_1 = L_1 - R_1(p_t^+ - p_t^-)/2. \tag{33a}$$

Similarly,

$$\bar{L}_2 = L_2 - R_2(p_t^+ - p_t^-)/2. \tag{33b}$$

The linear momentum of the target is, of course, always given by $P_2 = -P_1$. After substituting the definitions (Eqs. (26)) for p_r^+ and p_t^+ and (Eqs. (31)) for p_r^- and p_t^- into Eq. (32) we obtain, after q steps, half of which are in each direction, the following recursion relations for the average target linear momentum

$$\bar{P}_{1r}(q) = \bar{P}_{1r}(q-1)\left[1 - \tfrac{1}{2}\left(\frac{1}{A_1} + \frac{1}{A_2}\right)\right], \tag{34a}$$

$$\bar{P}_{1t}(q) = \bar{P}_{1t}(q-1)\left[1 - \tfrac{1}{2}\left(\frac{1}{A_1} + \frac{1}{A_2}\right)\right] - \tfrac{1}{2}\, m(\omega_1 R_1 + \omega_2 R_2). \tag{34b}$$

The last equation, (34b), can be simplified by expressing ω_1 and ω_2 in terms of angular momentum L_1 and L_2, via Eqs. (18) and (20). Then one obtains

$$\bar{P}_{1t}(q) = \bar{P}_{1t}(q-1)\left[1 - \tfrac{1}{2}\left(\frac{1}{A_1} + \frac{1}{A_2}\right)\right] - \tfrac{5}{4}\left(\frac{\bar{L}_1(q-1)}{R_1 A_1} + \frac{\bar{L}_2(q-1)}{R_2 A_2}\right). \tag{35}$$

We observe that Eqs. (33) can be simply written as

$$\bar{L}_1 = L_1 + (\bar{P}_{1t} - P_{1t})R_1 \tag{36a}$$

and

$$\bar{L}_2 = L_2 + (\bar{P}_{1t} - P_{1t})R_2. \tag{36bt}$$

Then after any number of steps q, half of which are in each direction, we obtain the average nuclear angular momenta in terms of the tangential component of the linear momentum, as follows:

$$\bar{L}_1(q) = L_1(0) + (\bar{P}_{1t}(q) - P_{1t}(0))R_1 \tag{37a}$$

and

$$\bar{L}_2(q) = L_2(0) + (\bar{P}_{1t}(q) - P_{1t}(0))R_2. \tag{37b}$$

From now on, $L_1(0)$ and $L_2(0)$ will be assumed to be zero, as is appropriate for reactions between even-even target and projectile nuclei.

Iterating (34a) back to the first transfer step we can express the radial component of the average linear momentum after q steps in terms of its initial value and obtain

$$\bar{P}_{1r}(q) = P_{1r}(0)\left[1-\tfrac{1}{2}\left(\frac{1}{A_1}+\frac{1}{A_2}\right)\right]^q. \tag{38}$$

To obtain the final expression for the tangential part of the average linear momentum, we substitute (37) into (35) to obtain

$$\bar{P}_{1t}(q) = \bar{P}_{1t}(q-1)\left[1-\tfrac{1}{2}\left(\frac{1}{A_1}+\frac{1}{A_2}\right)\right]-\tfrac{5}{4}P_{1t}(0)\left(\frac{1}{A_1}+\frac{1}{A_2}\right). \tag{39}$$

Combining the first two terms, iterating back to the first transfer step and summing the resulting geometrical series leads to

$$\bar{P}_{1t}(q) = P_{1t}(0)\left\{\tfrac{2}{7}\left[1-\tfrac{7}{4}\left(\frac{1}{A_1}+\frac{1}{A_2}\right)\right]^q+\tfrac{5}{7}\right\}. \tag{40}$$

After substituting (40) into (37) the expressions for angular momenta become:

$$\bar{L}_1(q) = \tfrac{2}{7}P_{1t}(0)\left\{\left[1-\tfrac{7}{4}\left(\frac{1}{A_1}+\frac{1}{A_2}\right)\right]^q-1\right\}R_1, \tag{41a}$$

$$\bar{L}_2(q) = \tfrac{2}{7}P_{1t}(0)\left\{\left[1-\tfrac{7}{4}\left(\frac{1}{A_1}+\frac{1}{A_2}\right)\right]^q-1\right\}R_2. \tag{41b}$$

3.2. Energy loss

The energy loss after q steps is defined by the difference between the initial kinetic energy of the relative motion and the kinetic energy after q steps,

$$E_{\text{loss}}(q) = E_k(0)-E_k(q). \tag{42}$$

$E_k(q)$ can be written directly in terms of the linear momentum $P(q)$ and reduces for $q = 0$ to

$$E_k(0) = \frac{1}{2\mu}(P_{1r}^2(0)+P_{1t}^2(0)), \tag{43}$$

where by (23),

$$P_{1t}^2(0)/2\mu = L^2/2\mu R_{12}^2, \tag{44}$$

and $L_0 \equiv L_{12}(0)$ is the initial relative angular momentum, equal here to the (conserved) total angular momentum of the system.

Then the energy loss can be written as

$$E_{\text{loss}}(q) = \frac{1}{2\mu}\left\{P_{1r}^2(0)\left[1-\left(1-\tfrac{1}{2}\left(\frac{1}{A_1}+\frac{1}{A_2}\right)\right)^{2q}\right]\right.$$
$$\left.+P_{1t}^2(0)\left[1-\left(\tfrac{2}{7}\left[1-\tfrac{7}{4}\left(\frac{1}{A_1}+\frac{1}{A_2}\right)\right]^q+\tfrac{5}{7}\right)^2\right]\right\}. \tag{45}$$

However, of this total energy loss from the relative kinetic energy, the amounts,

$$E_{\text{rot}}^1 = \frac{L_1^2(q)}{2I_1} \tag{46a}$$

and

$$E_{\text{rot}}^2 = \frac{L_2^2(q)}{2I_2} \tag{46b}$$

have been transferred into the rotational energy of the two nuclei, as required by conservation of angular momentum. Hence, the net energy dissipated to heat, E_{diss}, is seen to be correctly described by Eq. (7)

$$E_{\text{diss}}(q) = E_{\text{loss}}(q) - L_1^2(q)/2I_1 - L_2^2(q)/2I_2. \tag{47}$$

3.3. Rolling or sticking?

When nucleons are exchanged between the projectile and the target, angular momentum of the relative motion is transferred into the rotational angular momenta of the two nuclei. From the conservation of the linear momentum it follows, by virtue of Eqs. (18) and (37) that there exists, at each and every step, the following specific relation between the fragments' angular velocities; namely,

$$\omega_1 = \omega_2 R_2/R_1. \tag{48}$$

In contrast, the so-called "sticking" condition requires that all three angular velocities must be equal, $\omega_1 = \omega_2 = \Omega$. Hence, within the present RW transfer formalism, which leads to relation (48) between fragments angular velocities, the "sticking" condition can be satisfied if and only if $A_1 = A_2$, regardless of the number of steps.

On the other hand, the so-called "rolling" condition requires that

$$R_{12}\Omega = R_1\omega_1 + R_2\omega_2. \tag{49}$$

This condition is in fact approached for arbitrary values of A_1 and A_2 in the limit of a large number of steps, as we now demonstrate.

First, we re-write the left-hand side of Eq. (49) with the help of Eqs. (19) and (21) as

$$R_{12}\Omega = \frac{L_{12}}{\mu(R_1+R_2)}. \tag{50}$$

Similarly, using Eqs. (18), (19), and (20) we find that

$$R_1\omega_1 + R_2\omega_2 = \frac{2}{2m}\left(\frac{L_1}{A_1R_1} + \frac{L_2}{A_2R_2}\right). \tag{51}$$

Then from Eqs. (41) and (44) we obtain, as the number q of steps becomes large, the following limiting values for angular momentum L_1, L_2 and L_{12},

$$L_1^\infty = \tfrac{2}{7} L \frac{R_1}{R_1+R_2} \tag{52a}$$

and similarly,

$$L_2^\infty = \tfrac{2}{7} L \frac{R_1}{R_1+R_2}. \tag{52b}$$

Since the total angular momentum is conserved, Eq. (17) together with Eqs. (52) give

$$L_{12}^\infty = \tfrac{5}{7} L. \tag{53}$$

Therefore as $q \to \infty$, relations (50), (51), (52) and (53) imply that

$$\lim_{q\to\infty} R_{12}\Omega = \lim_{q\to\infty} (R_1\omega_1 + R_2\omega_2), \tag{54}$$

which is precisely the rolling condition of Eq. (49). Thus the system will always approach the rolling limit asymptotically as $q \to \infty$.

Since the total rotational energy of the system is given by

$$E_{\text{rot}} = \frac{L_1^2}{2I_1} + \frac{L_{21}^2}{2I_2} + \frac{L_{12}^2}{2I_{12}}, \tag{55}$$

we can also see from Eqs. (20), (52), and (53) that in this asymptotic rolling limit the amount of kinetic energy in the rotational motion of the two nuclei about their own axes and about their system center of mass is equal to

$$E_{\text{rot}}^\infty = \tfrac{5}{7} \frac{L^2}{2\mu R_{12}^2} = \tfrac{5}{7} \frac{P_{1t}^2(0)}{2\mu}. \tag{56}$$

Thus one finds that 5/7 of the initial tangential kinetic energy (44) is permanently unavailable for dissipation into random heat energy.

To check the $q \to \infty$ limit of the dissipated energy in Eq. (47) we use (52) first to express the limiting values of the fragments' rotational energies in Eq. (46) in terms of the initial tangential linear momentum $P_{1t}(0)$ via (44) and (20). This leads to

$$E_{\text{rot}}^{1\infty} + E_{\text{rot}}^{2\infty} = \tfrac{10}{49} \frac{P_{1t}^2(0)}{2\mu} = \tfrac{10}{49} \cdot \frac{L_0^2}{2\mu R_{12}^2}. \tag{57}$$

Also, the $q \to \infty$ limit of $E_{\text{loss}}(q)$ in Eq. (45) is given by

$$E^{\infty}_{\text{loss}} = \left\{ \frac{P^2_{1r}(0)}{2\mu} + \frac{P^2_{1t}(0)}{2\mu}\left(1 - \tfrac{2}{49}\right) \right\}, \tag{58}$$

so the limit of E_{diss} in (47) as $q \to \infty$ is

$$E^{\infty}_{\text{diss}} = \frac{P^2_{1r}(0)}{2\mu} + \tfrac{2}{7}\,\frac{P^2_{1t}(0)}{2\mu}, \tag{59}$$

which is consistent with Eq. (56) as is required by energy conservation. Since at least 5/7 of the tangential kinetic energy is tied up in the (minimal) rotational energy required to honor conservation of angular momentum, the dissipated energy must always be less than or equal to the sum of the remaining 2/7 of the initial tangential kinetic plus the initial radial energy. Thus the system tends towards the "rolling" configuration in which more kinetic energy is tied up in rotation, rather than towards the "sticking" configuration. Note that in the special case of $A_1 = A_2$ the two limits coincide. A more detailed discussion of these limits can be found in Ref. [6].

We note that for non-central collisions ($L \neq 0$) at a given bombarding energy, the kinetic energy available for dissipation is always less than for head-on ($L = 0$) collisions, by an amount equal to the minimal tangential kinetic energy required to honor the conservation of angular momentum. The smallest possible value of this rotational energy is given by the "rolling" $q \to \infty$ limit of Eq. (57). The maximal values of E_{loss}, E_{diss}, and of the energy dissipated per step, then all diminish monotonically with increasing values of L.

4. Results and discussion

The formalism presented in Sect. 3 has been applied to calculate various observables (the energy loss, the average values of the proton number, $\bar{Z}$, and of the neutron number, $\bar{N}$, in the projectile-like fragment, the total widths σ^2_A, σ^2_Z of the distribution, and the cut widths $\sigma^2_{Z|A}$ and $\sigma^2_{A|Z}$) as a function of the number of random walk steps, q. We have considered two different reactions, Fe+U at $E_{\text{lab}} = 464$ MeV and Fe+Ho at $E_{\text{lab}} = 464$ MeV for different values of the angular momentum L, keeping $\hat{T}_0$ of Eq. (2) constant at the value fitted to σ^2 for the $L = 0$ case [2].

The purpose is to provide some insight into the effect of angular momentum on such predictions, and the mechanism for such effects. For this purpose we shall first present the calculated results and discuss their general features. Afterwards, we shall turn to a more detailed discussion of the angular momentum effects.

Figures 2a and 2b present results for $E_{\text{loss}}(q)$ versus q for Fe+U and Fe+Ho, respectively, for several different values of L. It is obvious that, as mentioned in Sect. 3, both $E_{\text{loss}}(q)$ and the energy dissipated per step, dE_{loss}/dq, diminish monotonically with increasing values of L. The horizontal dotted lines in Fig. 2 show the "rolling" $q \to \infty$ limiting values of E_{loss} for the several values of L. Figures 3 to 8, respectively, show $\bar{Z}$, $\bar{N}$, σ^2_A, σ^2_Z, $\sigma^2_{A|Z}$ and $\sigma^2_{Z|A}$ for the Fe+U reaction and several values of L, as labelled, plotted as functions

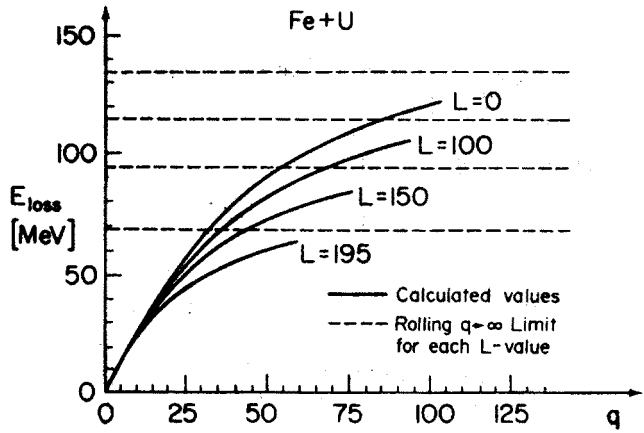

Fig. 2a. The calculated energy loss, E_{loss}, versus number of steps q for the reaction Fe+U at E_{lab} = 464 MeV, for angular momentum L = 0, 100, 150, and 195. The horizontal dotted line shows the limiting value of E_{loss} for each of the several values of L

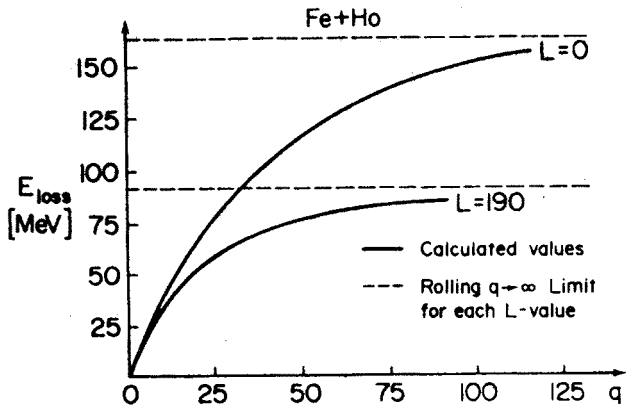

Fig. 2b. The same as in Fig. 2a for the Fe+Ho reaction at E_{lab} = 464 MeV, with L = 0 and L = 190

of the number of steps q. We notice that for all these quantities, as well as for E_{loss} and its slopes in Fig. 2, the results for different values of L remain essentially the same up to about 25 steps, corresponding to E_{loss} values of about 50 MeV.

For higher energy losses, the L-dependence for all the quantities studied is more pronounced. To analyze the source of this L-dependence, we consider the L-dependence of the transition probabilities of Eq. (1), which incorporate the physics of the random walk calculation. In general, the dependence of the various moments upon the transition probabilities is complicated, resulting from the solution of the RW equation. However, under the assumption that T_i's vary slowly over the range of evolving probabilities, the results simplify greatly. In Appendix A we show that the changes in the moments in the q^{th} step (equivalent to the derivatives with respect to q of these moments) can be expressed

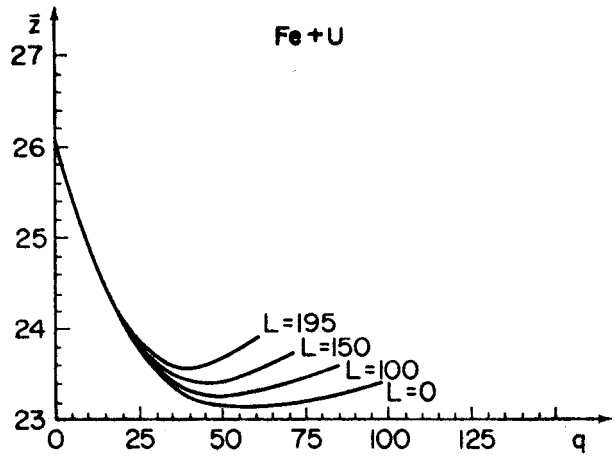

Fig. 3. The average number of protons $\bar{Z}$ in the projectile-like fragment for Fe+U at $E_{lab} = 464$ MeV for $L = 0, 100, 150, 195$, plotted vs number of steps q

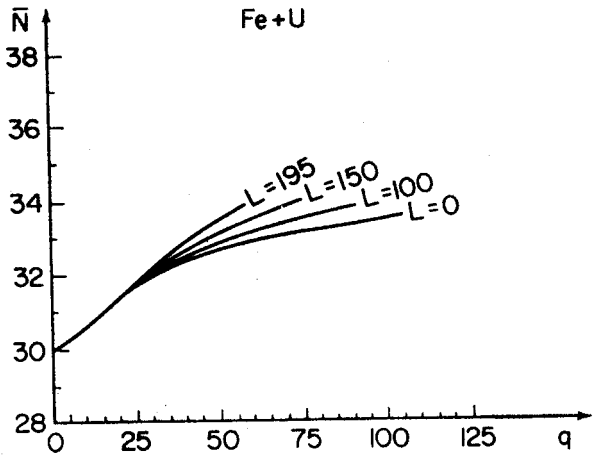

Fig. 4. The average number of neutrons $\bar{N}$ in the projectile-like fragment for the same reaction as in Fig. 3, plotted vs q

simply in the terms of averages of the transition probabilities, defined as follows:

$$\langle T_i \rangle_q \equiv \sum_{N,Z} T_i(N, Z) P_q(N, Z). \tag{60}$$

Specifically, we have shown that the first moments depend only upon average differences of the form $\langle T_1 - T_3 \rangle_q$, while the widths depend on the sums $\langle T_1 + T_3 \rangle_q$ and on differences only in the second order.

To ascertain the effect of angulat momentum upon Figs. 3–6, we must therefore inquire about the behavior of $\langle T_1 \pm T_3 \rangle_q$ and $\langle T_4 \pm T_2 \rangle_q$ with q for different angular momenta. In Appendix *B*, we consider these quantities as defined by the density of final states in terms

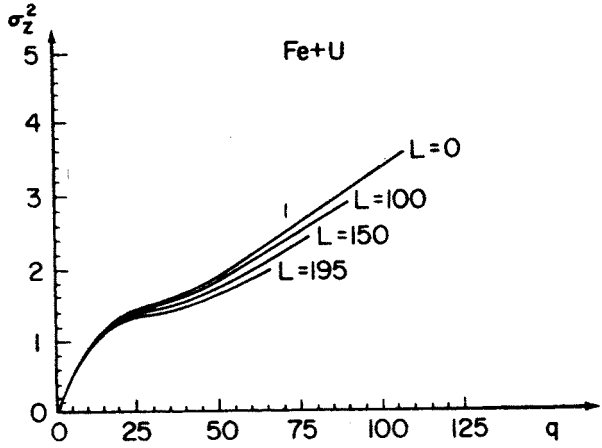

Fig. 5. The width σ_A^2 for the same reaction as in Fig. 3, plotted vs q

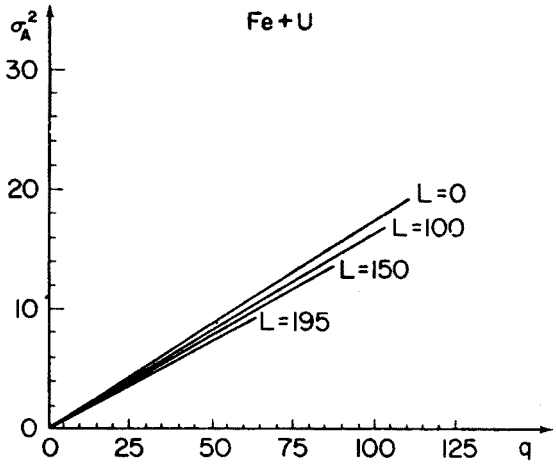

Fig. 6. The width σ_A^2 for the same reaction as in Fig. 3, plotted vs q

of the dissipated energy E_{diss} of Eq. (7) and the differences between neighboring ground state energies during the late stages of the evolution. We show there (*a*) that the sums of two transition probabilities vary much more slowly with E_{diss} than the differences, and (*b*) that for large values of E_{diss} the magnitude of the difference $|T_1 - T_3|$ diminishes monotonically with E_{diss} at every value of N and Z.

Since the dissipated energy, E_{diss}, at any specified value of q diminishes monotonically with increasing angular momentum, as exhibited in Figs. 2a and b, one can expect from these results of Appendix B that $|T_1 - T_3|$ and $|T_4 - T_2|$ are larger at a given q-value for large angular momenta than for small. Then at a sufficiently late stage of the evolution (which is to say, for large enough q-values), the slopes of $\bar{N}$ and $\bar{Z}$ in Eq. (A2a) should increase with increasing angular momentum (as in fact they do in Figs. 3 and 4), whereas

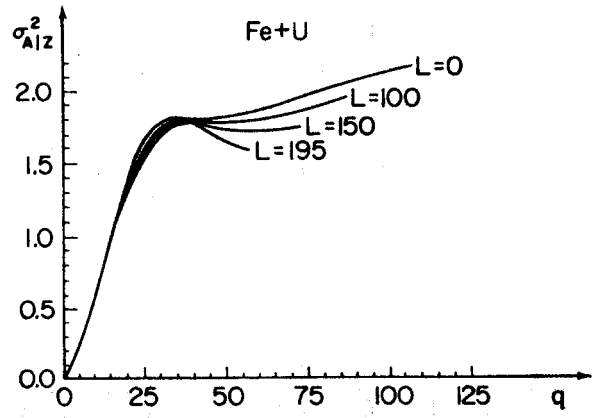

Fig. 7. The width $\sigma^2_{A|Z}$ for the same reaction as in Fig. 3, plotted vs q

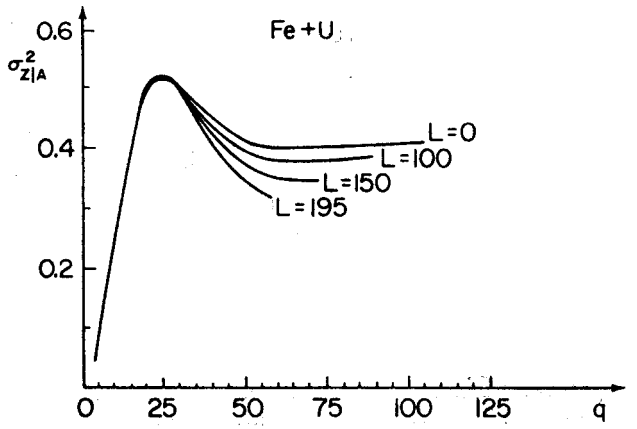

Fig. 8. The width $\sigma^2_{Z|A}$ for the same reaction as in Fig. 3, plotted vs q

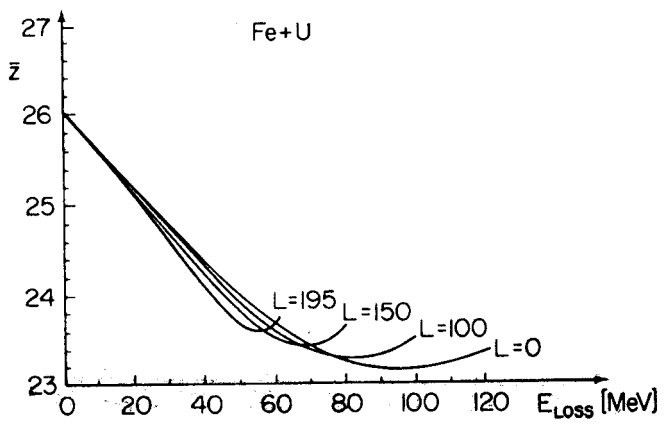

Fig. 9. Same as in Fig. 3, plotted vs E_{loss}

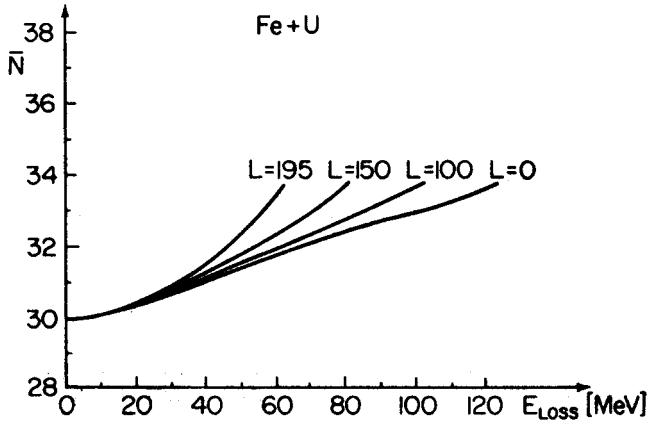

Fig. 10. Same as in Fig. 4, plotted vs E_{loss}

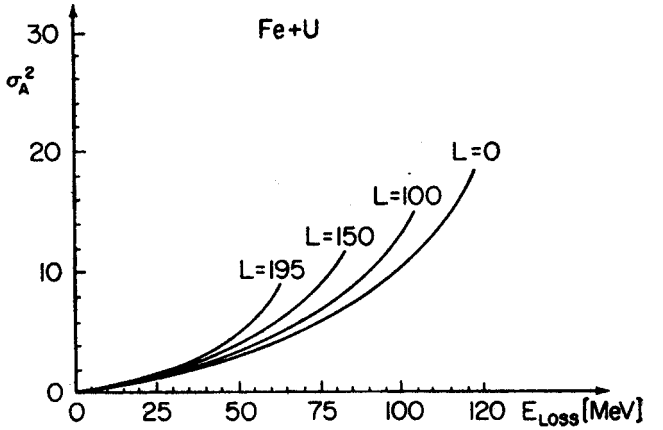

Fig. 11. Same as in Fig. 5, plotted vs E_{loss}

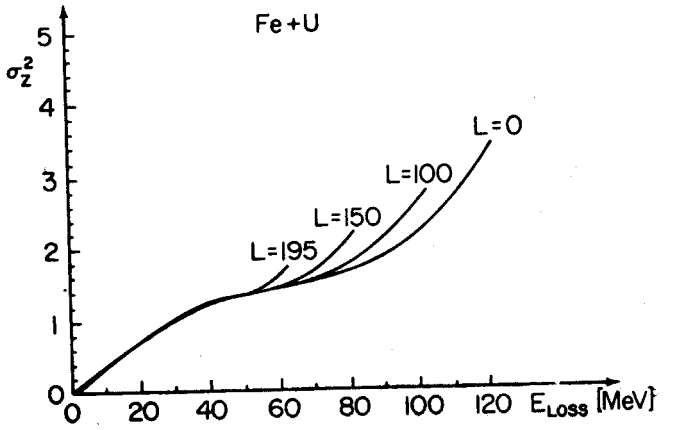

Fig. 12. Same as in Fig. 6, plotted vs E_{loss}

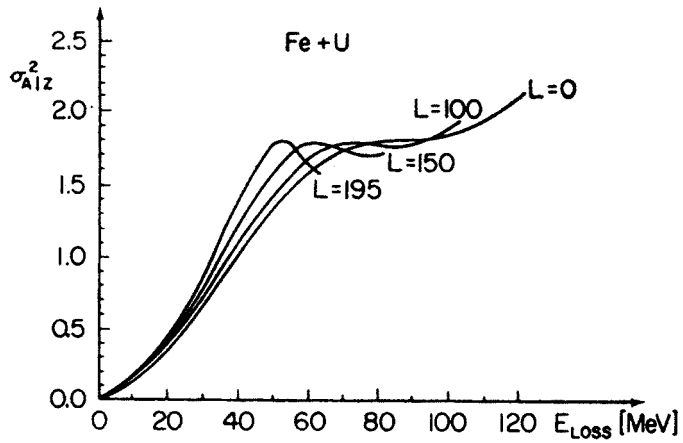

Fig. 13. Same as in Fig. 7, plotted vs E_{loss}

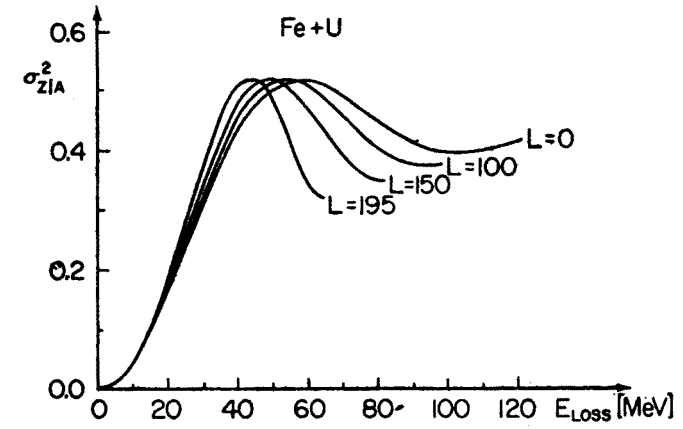

Fig. 14. Same as in Fig. 8, plotted vs E_{loss}

those of $\sigma^2(N)$, $\sigma^2(Z)$, $\sigma^2(N, Z)$ and $\sigma^2(A)$ should decrease with increasing angular momentum in accordance with Figs. 5 through 8.

One concludes [7] that the angular momentum dependence of the calculated q-dependent results presented in Figs. 3 through 8 behaves qualitatively as one would expect from the analyses leading to Eqs. (A1) through (A4). Beyond that, the angular momentum dependence of E_{loss} calculated as a function of q in Figs. 2 makes the results of $\bar{Z}$, $\sigma^2(Z)$, etc., vs E_{loss} (in Figs. 9 through 14) readily comprehensible as a combination of the simple L-dependence upon q of each such quantity and the nonlinear scale change from q to E_{loss} given by Figs. 2.

In short, the various numerical calculations presented here are all consistent with the view that the effect of angular momentum upon the q-dependences of the various physical observables is small and arises implicitly through the dependence of the transition probabilities upon the energy loss, whose dependence upon angular momentum is chiefly re-

sponsible for the calculated angular momentum dependence of $\bar{N}$, σ_N^2, ... etc. On the other hand, the angular momentum dependence of various quantities as functions of E_{loss} itself is somewhat stronger due to the nonlinear angular momentum dependence of E_{loss} on q. In particular, a RW calculation which assumes throughout that the angular momentum is zero is reasonably accurate both at small energy losses (corresponding in the physical reaction to large values of the angular momentum) because of the insensitivity there to angular momentum, and at larger energy losses, where the small angular momentum assumption actually corresponds well with the physical reality.

The support of the U.S. Department of Energy for this research is gratefully acknowledged. MZP and MD would like to express their gratitude to the Nuclear Theory Group of the University of Maryland in College Park for their support and hospitality during their stay there.

APPENDIX A

Expressions for various moments in terms of averaged transition rates

The relationship between the transition probabilities and the average values of such quantities as N, Z, N^2, NZ, etc., which define the measured quantities calculated in the figures can be quantified by considering the amount $\Delta\langle M\rangle_q$ by which the average value $\langle M\rangle$ changes in the q^{th} nucleon transfer, as follows:

$$\Delta\langle M\rangle_q = \langle M\rangle_q - \langle M\rangle_{q-1} = \sum_{N'Z'} M(N', Z')\,[P_q(N', Z') - P_{q-1}(N', Z')], \tag{A1a}$$

$$\Delta\langle M\rangle_q = \sum_{N'Z'} M(N'Z')\Delta P_q(N'Z). \tag{A1b}$$

Then Eq. (1) provides the expression for $\Delta P_q(N', Z')$ in terms of the transition probabilities, $T_i(N', Z')$, and one can calculate the following exact specific results,

$$\Delta\langle N\rangle_q = \langle T_1 - T_3\rangle_{q-1} = \sum_{N'Z'} [T_1(N', Z') - T_3(N', Z')]P_{q-1}(N', Z'), \tag{A2a}$$

$$\Delta\langle N^2\rangle_q = \langle T_1 + T_3\rangle_{q-1} + 2\langle N\rangle_{q-1}\langle T_1 - T_3\rangle_{q-1} + 2\langle (N - \langle N\rangle_{q-1})\,(T_1 - T_3)\rangle_{q-1}, \tag{A2b}$$

$$\Delta\langle NZ\rangle_q = \langle Z\rangle_{q-1}\langle T_1 - T_3\rangle_{q-1} + \langle N\rangle_{q-1}\langle T_4 - T_2\rangle_{q-1}$$

$$+ \langle (Z - \langle Z\rangle_{q-1})\,(T_1 - T_3) + (N - \langle N\rangle_{q-1})\,(T_4 - T_2)\rangle, \tag{A2c}$$

with corresponding results, in which $(T_4 - T_2)$ and $(T_4 + T_2)$ replace $T_1 + T_3$ when Z replaces N. If the transition probabilities are nearly constant, then the last terms in (A2b) and (A2c) can be neglected, and the quantities

$$\langle T_1 \pm T_3\rangle_{q-1} = \sum_{N'Z} P_{q-1}(N', Z')\,[T_1(N', Z') \pm T_3(N', Z')] \tag{A3}$$

determine these various increments at the q^{th} nucleon transfer, and therefore the slopes of the curves in Figs. 3 through 6.

In particular, for $\sigma_q^2(N)$ and $\sigma_q^2(Z)$ the results (A2) imply that

$$\Delta\sigma_q^2(N) = \langle T_1+T_3\rangle_{q-1}+2\langle N\rangle_{q-1}\langle T_1-T_3\rangle_{q-1}^2+2\langle(N-\langle N\rangle_{q-1})(T_1-T_3)\rangle_{q-1} \tag{A4a}$$

with an analogous result for $\sigma_q^2(Z)$. Also, for $\sigma_q^2(A)$, we find

$$\Delta\sigma_q^2(A) = \langle T_1+T_2+T_3+T_4\rangle_{q-1}-\langle T_1-T_3+T_4-T_2\rangle_{q-1}^2$$
$$+2\langle(A-\langle A\rangle_q)(T_1-T_3+T_4-T_2)\rangle_{q-1}. \tag{A4b}$$

In Eqs. (A4) we again neglect the final terms on the assumption that the T_i's vary slowly over the range of the evolving probability distribution. Note also that the normalization condition (4) implies that in Eq. (A4b)

$$T_1+T_2+T_3+T_4 = 1-T_0 = 1-\gamma. \tag{A5}$$

We note that the results (A1) through (A5) reduce immediately to the exact model results of Table 2 of Eef. [8], under the assumption made there that all $T_i(N, Z)$ are constant, independent of N and Z.

APPENDIX B

Angular momentum dependence of averaged transition rates

In this appendix we consider the quantities $\langle T_1+T_3\rangle$ and $\langle T_1-T_3\rangle$ which occur in the expressions (A1) through (A4) for the increments of the various physical observables. We find that for sufficiently large values of the dissipated energy, the former quantity approaches a constant while the latter diminishes to zero as $(E_{\text{diss}})^{-1/2}$.

Since this is true at every value of N and Z, it is also true for the averaged values, $\langle T_1+T_3\rangle_q$ and $\langle T_1-T_3\rangle_q$, which determine the behavior of $\Delta\langle N\rangle_q$, $\Delta\sigma_q^2(N)$, etc., in the equations cited, provided only that the distributions $P_q(N, Z)$ are not too different for the situations compared. Since in particular we wish to compare situations corresponding to different values of the angular momentum, the relatively small differences calculated among the various angular momentum values at a given q-value in Figs. 3 through 8 tends to corroborate this assumption. If in addition the transition rates are changing slowly over the width of the distribution, the tendency for the magnitude of these quantities simply to scale inversely with the dissipated energy is enhanced.

We consider the transition probabilities defined by Eqs. (3)–(6), upon which all of our numerical calculations herein are based. In particular, we consider the quantities, $R^{\mp}$, proportional respectively to the difference, T_1-T_3, and the sum, T_1+T_3:

$$R^{\mp} = \frac{T_1\mp T_3}{(1-\gamma)} = \frac{\{e^{\sqrt{a(E_{\text{diss}}-E_1)}}\pm e^{\sqrt{a(E_{\text{diss}}-E_3)}}\}}{e^{\sqrt{a(E_{\text{diss}}-E_1)}}+e^{\sqrt{a(E_{\text{diss}}-E_3)}}+e^{\sqrt{a(E_{\text{diss}}-E_2)}}+e^{\sqrt{a(E_{\text{diss}}-E_4)}}}, \tag{B1}$$

where the T_α are given by Eq. (4), $a = \pi^2 A/\varepsilon_F = (\pi^2 A/37)\,\mathrm{MeV}^{-1}$, and E_α is the ground state energy of the nuclei at the locations $(N, Z)+\Delta_\alpha$ with respect to the ground state energy of the injection point, and hence is of the order of a few MeV. Also, for simplicity we have neglected the slow $(E^*)^{5/4}$ dependence on E^* from each of the exponentials of Eq. (5). We first expand all of the exponents in the small parameter E_i/E_{diss}, keeping only the leading terms. This leads to

$$R^{\pm} = \frac{1 \pm e^{-1/2(E3-E1)/\mathscr{E}}}{\sum_i e^{-1/2(Ei-E1)/\mathscr{E}}}, \tag{B2}$$

where $\mathscr{E} = (E_{\mathrm{diss}}/a)^{1/2}$ is the relevant measure of the dissipation energy. Then in the limit of the very large E_{diss}, the quantities $(E_1 - E_3)/\mathscr{E}$ can be considered small and the expansion of the exponentials leads to the following simple form:

$$\lim_{E_{\mathrm{diss}} \to \infty} R^+ = 1/2[1+(E_2+E_4-E_1-E_3)/8\mathscr{E}+\mathcal{O}(\mathscr{E}^{-1}) \ldots] \tag{B3a}$$

and

$$\lim_{E_{\mathrm{diss}} \to \infty} R^- = (E_3-E_1)/8\mathscr{E}+\mathcal{O}(\mathscr{E}^{-2}). \tag{B3b}$$

Then at every value of N and Z, the quantity (T_1+T_3) approaches a constant for large values of E_{diss}. It follows that the average, $\langle T_1+T_3\rangle_q$, also approaches the same constant, by virtue of the fact that $P_q(N, Z)$ is normalized to unit probability. This result guarantees that $\langle T_1+T_3\rangle$ terms in Eqs. (A2) and (A4) are essentially independent of q and of E_{diss} for large enough values of E_{diss}.

The quantity, $|T_1-T_3|$, on the other hand, diminishes as $\mathscr{E}^{-1}$ at every value of N and Z for large values of E_{diss}. One therefore must expect that the magnitude of its average, $\langle T_1-T_3\rangle_q$, would tend to also decrease with increasing E_{diss}, unless the probability distribution is shifting in such way as to alter the proportionate contributions from positive and negative values of T_1-T_2. (We note that precisely such a behavior when $\langle T_4-T_2\rangle_q$ changes sign in the range $35 < q < 60$, as indicated by the slopes of $\bar{Z}$ vs q in Fig. 3.) Then, apart from such special circumstances, we expect that the magnitude of $\langle T_1-T_3\rangle$ (and $\langle T_4-T_2\rangle$) will diminish as (a large value of) E_{diss} increases.

Since E_{diss} at any given q-value always diminishes with increasing angular momentum (as shown in Figs. 2), one expects the magnitude of $\langle T_1-T_3\rangle_q$ and $\langle T_4-T_2\rangle_q$ to increase (because $E_{\mathrm{diss}}(q)$ is diminishing) with increasing L at large enough values of E_{diss}. This expectation together with Eqs. (A2) and (A4) for the slopes of the various observables conforms to the L-spreads actually calculated at high q and exhibited in Figs. 3 through 6.

Editorial note. This article was proofread by the editors only, not by the authors.

REFERENCES

[1] J. J. Griffin, Y. Boneh, K.-K. Kan, M. Dworzecka, *Nucl. Phys.* **A369**, 181 (1981).
[2] J. J. Griffin, Y. Boneh, M. Dworzecka, K.-K. Kan *Nucl. Phys.* **A382**, 159 (1982).
[3] A. Gökmen, M. Dworzecka, J. J. Griffin, *Nucl. Phys.* **A440**, 586 (1985).
[4] Y. Boneh, M. Dworzecka, K.-K. Kan, J. J. Griffin, U. of Md. PP #81-238 (1981).

[5] W. D. Myers, W. J. Swiatecki, *Ann. Phys. (N. Y.)* **55**, 395 (1969); W. D. Myers, *Nucl. Phys.* **A145**, 387 (1970).
[6] L. G. Moretto, G. J. Wozniak, LBL-17426 (1984).
[7] M. Dworzecka, M. Zielinska-Pfabé, J. J. Griffin, Proc. IVth Winter Workshop on Nuclear Dynamics, Copper Mountain, Colorado, U. of Md. ORO #5126–280 (1986).
[8] B. Hiller, A. H. Blin, M. Dworzecka, J. J. Griffin, *Nucl. Phys.* **A424**, 335 (1984).